Astrophys. Space Sci. Trans., 7, 411–416, 2011
www.astrophys-space-sci-trans.net/7/411/2011/
doi:10.5194/astra-7-411-2011

ASTRA
Astrophysics and Space Sciences Transactions

Measurement of high-energy neutrons at ISS by SEDA-AP

K. Koga[1], T. Goka[1], H. Matsumoto[1], T. Obara[1], Y. Muraki[2], and T. Yamamoto[3]

[1]Tsukuba Space Center, JAXA, Tsukuba, Japan
[2]Solar-Terrestrial Environment Laboratory, Nagoya University, Nagoya 464-8601, Japan
[3]Department of Physics, Konan University, Kobe 658-8501, Japan

Received: 11 September 2010 – Revised: 3 March 2011 – Accepted: 4 March 2011 – Published: 20 September 2011

Abstract. A new type of solar neutron detector (NEM) was launched by the space shuttle Endeavour on 16 July 2009 and it began collecting data on 25 August 2009 at the International Space Station (ISS). In this paper we introduce preliminary results obtained by the NEM.

1 Introduction

The Space Environment Data Acquisition equipment - Attached Payload (SEDA-AP) detector was first proposed for the measurement of radiation levels at the International Space Station (ISS) in 1991. It was designed as one of the detectors onboard the Japan Exposure Module, JEM-ISS. It comprises not only a neutron detector (NEM) but also various other detectors such as charged particle detectors (HIT and SDOM), a plasma detector (PLAM), an atomic oxygen monitor (AOM), electronic device evaluation equipment (EDEE and SEED) and the system even includes a micro-particle capture detector (MPAC). The MPAC and SEED have been returned back to Earth by the astronauts. Technical details can be found on the JAXA Website http://kibo.jaxa.jp/en/experiment/ef/seda-ap.

As one of the components of the SEDA-AP, the NEM can be extended 1 m away from the main frame by means of a mast in order to measure solar neutrons under low-background conditions. The system has a 220 watt power supply and a total weight of 450 kg. Although the official mission lifetime has been estimated to be 3 years, given the importance of the measurements, it would be highly desirable to extend this to cover at least one solar cycle of 11 years, if the system continues to operate.

Correspondence to: Y. Muraki
(muraki@konan-u.ac.jp,
muraki@stelab.nagoya-u.ac.jp)

Before giving technical details of the system, we will first provide a brief history of the SEDA-AP until its launch. Between December 1991 and March 1992, an advisory board was formed to consider methods of studying the radiation environment in space. It was composed of representatives from universities and companies in addition to NASDA (presently JAXA) members. The committee first considered all parameters influencing the long-term operation of the ISS and how accurately these could be measured. At the request of the users, 20 such subjects were proposed by the committee.

In 1994, a 19-member frontier study group was assembled from universities, companies and NASDA, to focus mainly on the following research items: (1) detectors for the measurement of the space environment, (2) data analysis, ground tests and modeling of the space environment and (3) the effect of the local space environment on the components of the satellite. The original 20 parameters to be monitored were narrowed down to 11 at this point. In addition, it was decided that neutron measurements should be given the highest priority. A proposal was written immediately and sent to the government selection committee. In April 1997, the subject of space measurements was selected by the committee to be studied during the initial stage of the JEM-ISS (Chikaoka, 1997).

In 2001, the flight module (FM) was ready to be deployed (Fig. 1), but due to a space shuttle accident, it had to be stored in a special clean room for 8 years until it could finally be launched. The FM was launched by the space shuttle Endeavour on 16 July 2009 and began taking measurements 25 August 2009.

2 Scientific Goal

There are three main scientific goals in this experiment.

(1) Accurate measurements of radiation levels in the environment of the ISS. It had been estimated that astronauts

Published by Copernicus Publications on behalf of the Arbeitsgemeinschaft Extraterrestrische Forschung e.V.

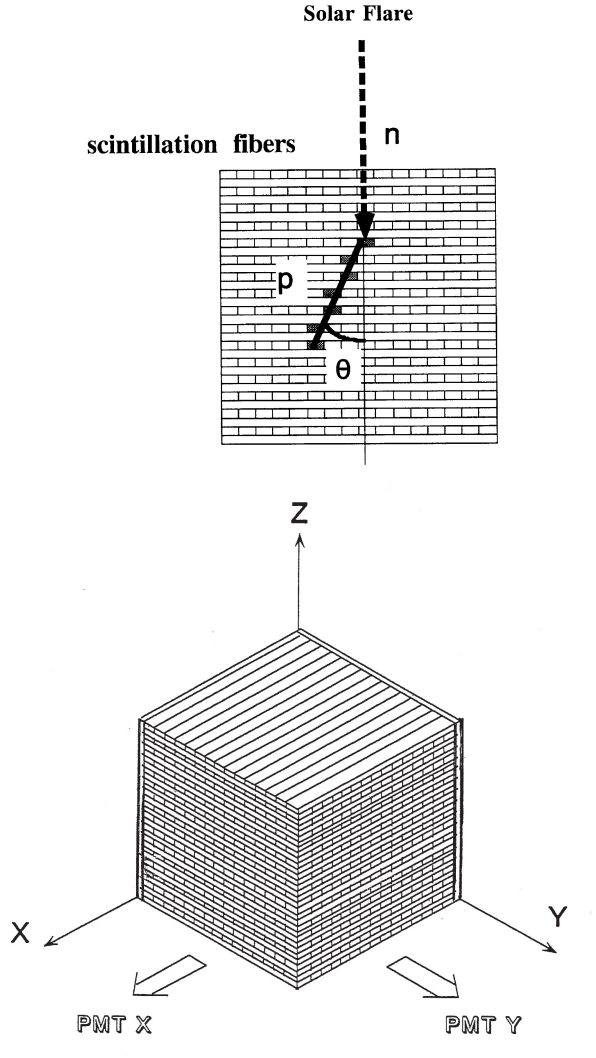

Fig. 1. The schematic view of the FIB sensor of NEM. **(a)** top: The FIB detectors consist of 16 layers of 16 sticks of the scintillation bars. Method of energy determination of neutrons by kinematics is schematically shown. **(b)** bottom: The alignment of the scintillation bars. Each layer is located alternatively along the x-direction and y-direction. The positions of the two photomultipliers PMT X and PMT Y are also indicated. The sensor is surrounded by the 6 plates of the scintillator and they are used for the anti-counter.

who stay on the ISS for one year receive an equivalent radiation dose of 300 mSy during quiescent solar periods (Doke, 1997). However, no precise data was available for neutrons, and measurement of the neutron background at the ISS was thus a high-priority task.

(2) Rapid prediction of the imminent arrival of large numbers of charged particles from the Sun by monitoring neutron levels. Such particles are produced by large solar flares and are transported to the Earth by the interplanetary magnetic field. Since they are trapped in the magnetic field, they arrive at the Earth a few hours later than the light associated with the flare. They are sometimes observed by the ground level detectors and known as Ground Level Enhancements.

It of course depends on the position of the flare on the solar surface and the momentum of charged particles, but according to the observation by GOES satellite, even in the quickest case these particles lag the light by about 20 min (Chinnery, 1989)[1]. However, since neutrons do not interact with the magnetic field, they arrive at Earth's upper atmosphere earlier than the charged particles. Thus, if a large X-class solar flare is detected by the GOES satellite, and is immediately followed by an increased neutron flux in the vicinity of the ISS, then the arrival of a large number of charged particles can be predicted. This would allow the astronauts working on the ISS to take preventative measures by remaining behind a thick aluminum wall until the charged-particle storm has passed. Thus, this corresponds to space weather forecasting.

(3) The establishment of an acceleration model for charged particles above the solar surface is an important issue in cosmic-ray physics. We wish to know when and how these particles are accelerated. When they finally arrive at Earth and are detected, important information may be lost concerning the timing of their departure from the Sun. To identify the acceleration mechanism of particles at the Sun, it is necessary to compare the data of neutral particles with images taken by a soft X-ray telescope.

We can illustrate this 3rd point using historical data first recorded by the ground-based solar neutron detector located at Jungfraujoch, Switzerland on 3 June 1982 (Chupp et al., 1987). The event was also recorded by the SMM satellite. An interesting feature in the Jungfraujoch data, shown in Fig. 2, bottom, is that a main peak was observed at 11:45 UT and was followed by a tail extending to 12:04 UT. In particular, the arrival of neutrons after 11:57 UT poses an interesting problem concerning the particle acceleration mechanism.

Since they have mass, even neutrons emitted at the same time from the Sun will have different arrival times at the Earth, depending on their energy. However, not all of these neutrons will be energetic enough to penetrate Earth's atmosphere. In particular, the Monte Carlo calculations of Shibata (1994) showed that solar neutrons with energies less than 100 MeV will be absorbed by the atmosphere, and so can not be detected by ground-based stations. Solar neutrons with an energy of 100 MeV will arrive at Earth 11 min behind the light wave front. Therefore, the peak before 11:55 UT on 3 June 1982 can be attributed to the instantaneous production of solar neutrons at 11:43 UT. However, the long tail after 11:55 UT cannot be explained by this mechanism since such late-arriving neutrons would be expected to have insufficient

[1]In the occasion of one of the hardest solar flare event observed in 29 September 1989, an increase of events was observed after 30 min later than the peak time of Xrays by one of the channels of the GOES sensor in the range of $Ep = 640\,\mathrm{MeV} - 850\,\mathrm{MeV}$

energy to penetrate the atmosphere. This suggests that there may be an additional acceleration mechanism involved.

To determine the particle acceleration mechanism at the Sun, and distinguish between neutrons that are being continuously produced and those that are spontaneously generated in events such as solar flares, it is essential to employ a new type of neutron detector that can measure the energy of neutrons. Until now no such detector has been launched into space, although the ground-based Solar Neutron Telescope (SONTEL) has being operating for a number of years (Bütikofer et al., 2001; Gonzalez et al., 2010; Muraki et al., 2007). Thus, the NEM-FIB detector installed in the SEDA-AP is the first attempt at meeting the challenge of neutron energy measurement in space.

3 Detector design, performance and trigger

In order to achieve the scientific goals listed earlier, a fine-grated neutron detector (referred to as the FIB detector) has been designed. It consists of a 16×16 stack of scintillation bars, each with dimensions of $3\,\text{mm} \times 6\,\text{mm} \times 96\,\text{mm}$ (length). An optical fiber is coupled to the end of each bar to collect photons produced in the scintillator. These are sent to a 256-channel multi-anode-photomultiplier (Hamamatsu H4140-20). A schematic image of the FIB detector is shown in Fig. 2. It measures the tracks of recoil protons produced by incident neutrons and determines the neutron energy using the range method.

It can also identify the direction of neutron incidence. Discrimination between neutrons and protons is achieved by an anti-coincidence system comprising 6 scintillator plates surrounding the FIB sensor in a cubic arrangement. The effectiveness of the anti-coincidence system in rejecting signals due to charged particles was evaluated using the accelerator beam at Riken. The FM was irradiated with a charged particle beam with an intensity of one million particles/sec and an energy of 160 MeV/n. No neutron detection event was identified by the internal sensor. However, when an aluminum target was placed in front of the module, the sensor immediately began to identify neutron signals. Actually we are taking the neutron data over SAA. The counting rate of the anti-coincidence system at SAA is 60 000 counts/sec (at the maximum) and it works.

We use the range method to estimate the energy of the neutrons. Neutrons are converted into protons via a charge-exchange process when they collide with the hydrogen target in the plastic scintillator. The momentum of the incoming neutrons is transferred to these protons. In the case of solar neutrons, the direction of the source (the Sun) is known, so we can measure the momentum of incoming solar neutrons. Let us assume the angle between the trajectory of the recoil protons and the incident neutron direction as θ (Fig. 1**(a)**). Then the energy of the incoming neutrons (En) can be uniquely determined using the equation

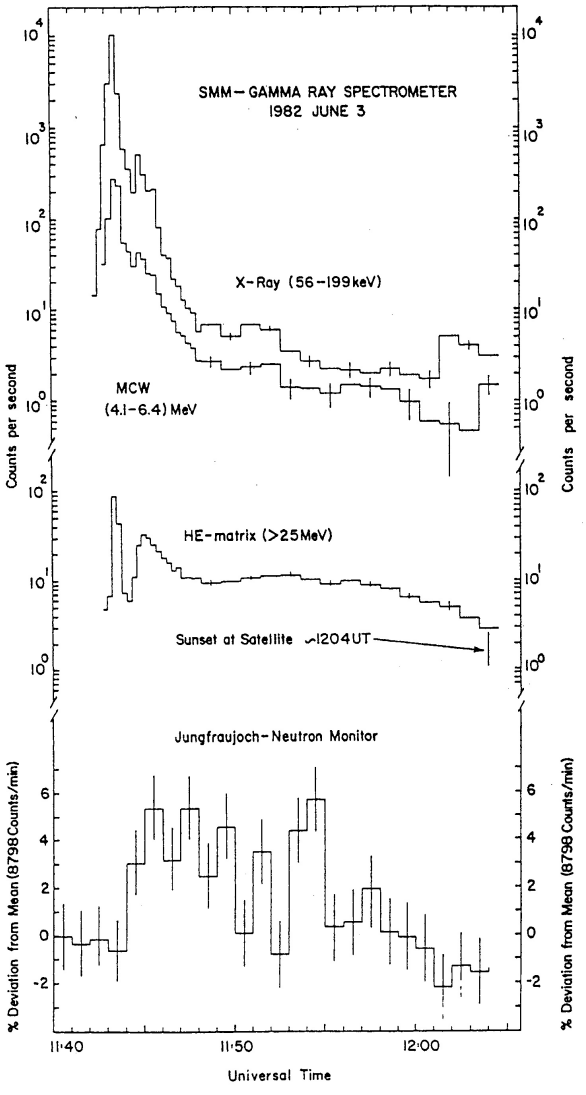

Fig. 2. The time profile of the event observed by the Gamma-Ray Spectrometer (GRS) of the Solar Maximum Mission (SMM) and Jungfraujoch neutron monitor (bottom) in association with the solar flare of 3 June 1982. From the top to the bottom, the data represent for hard X-rays ($56-199\,\text{keV}$), line gamma rays ($4.1-6.4\,\text{MeV}$), high energy gamma-neutron data ($>25\,\text{MeV}$) observed by the GRS detector onboard SMM satellite and high energy neutrons detected at Jungfraujoch neutron monitor. The HE-matrix data shows an interesting feature of the event, the first peak corresponds to gamma-rays and the second enhancement may correspond to photons and/or neutrons, and the third bump must represent low energy neutrons.

$En = Ep/(\sin\theta)^2$, if we assume an n-p scattering process. Here Ep represents the energy of the recoiled protons. Details of the detector have been published elsewhere (Koga et al., 2008, 2009).

The neutron detector has a cubic shape with sides of 10 cm. The maximum measurable momentum is about

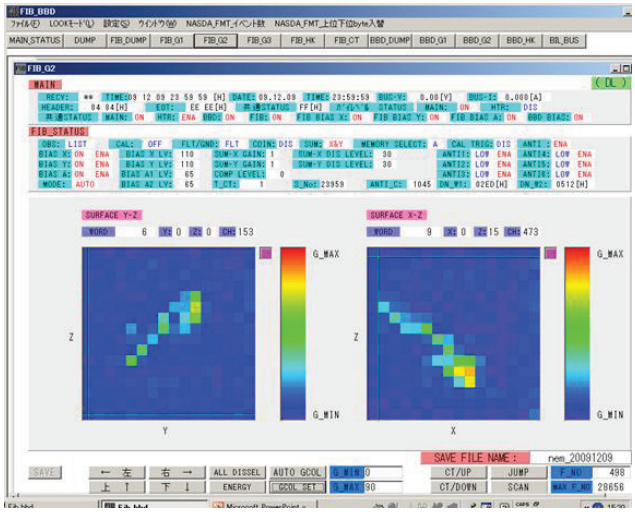

Fig. 3. A typical example of a neutron event. A neutron enters into the upper part of the sensor from the main body of ISS. Left side screen represents the track seen from the $-y$ direction ($y-z$ plane), while the right side screen shows the track observed from $-x$ direction ($x-z$ plane).

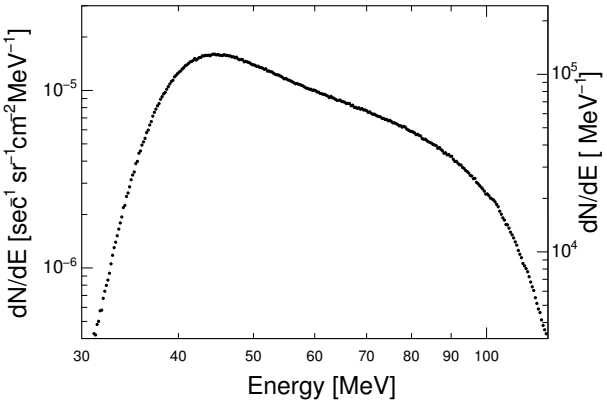

Fig. 4. Secondary proton spectrum induced by neutrons observed by the NEM-FIB sensor. The data have been taken during the flight between 1 January 2010 and 31 July 2010. The differential intensity of protons is given in the right side of the ordinate, while the differential spectrum of secondary protons is given in the left side of the ordinate by the unit of particles/s $\cdot$ sr $\cdot$ cm$^2\cdot$ MeV

.

120 MeV/c. The sensor is monitored from two directions by two multi-anode photomultipliers and the arrival direction of the tracks can be identified. To determine the arrival direction of neutrons, protons must penetrate at least four layers of the scintillating bars, each of which consists of 3 mm-thick plastic bars. This corresponds to 35 MeV as the lowest momentum of protons that can identify the direction. The one layer of the detector consists of 16 pieces of scintillating bars, and each layer is located alternatively along the x-axis and y-axis. A schematic view is given in Fig. 1**(b)**.

Here we discuss the neutron detection efficiency of this detector. Since the detector has a cubic shape with sides of 10 cm, if neutrons with kinetic energy higher than 120 MeV interact at the top of the detector, the track of protons will be fully contained in the apparatus. However, if the n-p scatterings occur in the lower part of the detector, the recoil protons will escape it crossing one anti-counter plane. Therefore the anti-counter is triggered and the neutron event will be not recorded. This results in an energy-dependent geometrical factor. Furthermore, the nuclear interaction cross-section also depends on the energy of the neutrons, which introduces a further energy dependence in the detection efficiency (Moser et al., 2005)[2].

Actually we have obtained the correction efficiency ϵ by the Monte Carlo method, using the Geant4 program. In this calculation, the collisions between neutrons and carbon target are also taken into account. The detection efficiency of neutrons for vertical incidence can be approximated by $\epsilon = 3.45 \times E\,\mathrm{MeV}^{-0.7118}$. For the incidence with $\theta = 10°$, 20° and 30°, the coefficient (3.45) are replaced by 3.1, 2.9 and 2.6, respectively.

In the data analysis, another condition has been applied; the minimum energy deposited in the sensor exceeds 35 MeV. According to the Monte Carlo calculation, the detection efficiency ϵ can be expressed by $\epsilon = 1.15 \times (E\,[\mathrm{MeV}] - 25) \times E\,[\mathrm{MeV}]^{-1.8}$. In fact the detection efficiency ϵ could be approximated by a constant value 0.021 (almost 2%) in the energy range of incident neutrons $En = 50-120$ MeV.

On the other hand, the Monte Carlo calculation tells us that the secondary proton spectrum with $Ep > 35$ MeV induced by primary neutrons in the sensor can be well described by a simple relation as $(Ep/En)^{-1.5}$. Then the secondary proton spectrum Ip presented in Fig. 4 can be related with the primary spectrum of neutrons by the relation:

$$Ip(>Ep) = A\int_{Ep}^{\infty} En^{-\gamma}\left(\int_{E*}^{En}(Ep/En)^{-1.5}dEp\right)dEn$$
$$= AEp^{2-\gamma}/(2-\gamma)(2.5-\gamma), \quad (1)$$

where Ep should be higher than $E* = 35$ MeV.

The proton spectrum given in Fig. 4 can be fit by a power law in the energy range of $Ep = 45-85$ MeV with the differential power index of -1.75 or the integral power index -0.75 (Eq.B). In comparison with Eqs. (1) and (B) , the γ should be 2.75 ($2-\gamma = -0.75$). This is an expected differential spectral index for primary neutrons from ISS. But

[2]For the n-p scattering process, the cross-section can be treated analytically. The correction factor is the product of a geometrical factor and a nuclear interaction factor. The correction factor is given by $(1.0-0.8\times(E_p/100\,\mathrm{MeV})^{1.82})$(geometrical) $\otimes(0.375\times(E_n/100\,\mathrm{MeV})^{-0.81})$ (interaction). The n-p cross section was measured in an accelerator experiment and was determined to be 14 mb/sr in the forward region at 92 MeV.

Eq. (1) has been derived under the condition that differential index of primary neutrons must be softer than 2.5. For the different case the analytic estimation is difficult, therefore we need another Monte Carlo calculation. In this paper we only provide the flux of observed protons. The differential spectrum of protons (the left side ordinate of Fig. 4) has been obtained by dividing the energy spectrum (presented in the right side of the ordinate) by the total observation time ($T = 1.74 \times 10^7$ s and the effective acceptance of the detector ($S\Omega = 50\,\mathrm{cm}^2$ str). Here we have assumed the solid angle of the detector toward the ISS is 0.5 steradian. The data are presented in Fig. 4 for regions excluding the SAA.

We measured the energy resolution of the sensor using the Riken proton beam and obtained a value of $\Delta E/E = \left(14/\sqrt{E_p/100\mathrm{MeV}} - 10.3\right)\%$. For example, the detector has an energy resolution of 4% at $E_p = 100$ MeV and 13% at $E_p = 36$ MeV. The details have been published elsewhere (Imaida et al., 1999).

Below 15 Hz of the trigger rate, both the range and the direction of the generated protons can be measured. Above this frequency, the system cannot obtain information on proton tracks, and the incident neutron flux is recorded based on the dynode signals alone. The question that arises is, when a large solar flare occurs producing neutrons at the solar surface, will it be possible to measure the tracks of all neutrons? Based on the results of our previous Monte Carlo simulations (Imaida et al., 1999; Watanabe, 2005) of large flares such as those that occurred on 4 June 1991 and 24 May 1990, it would be possible to record the tracks of the high energy neutrons arriving within 1100 s after the flare. However, following this, track information will not be obtainable. The cutoff neutron energy was calculated to be less than 50 MeV. However, for other flares such as those that occurred on 22 March 1991, 24 November 2000 and 28 October 2003, the sensor would be capable of recording the tracks of all arriving neutrons during the entire event.

4 Measurement of neutrons at ISS

Here we report actual neutron measurement results at the ISS. Figure 3 shows a typical event detected by the NEM sensor. The right side image was taken by the PMT located at the leading section of the ISS ($x-z$ plane) and the left side image presents a photo taken from the down side of the sensor ($y-z$ plane), i.e. looking away from the Earth. The $y-z$ sensor is pointing away from the Earth (in the FIB local coordinate system). The x-direction is defined as towards the center of the Earth, the ISS advances along the $-y$-direction and the SEDA-FIB detector is pointing along the $-z$ direction in the pressurized module. The color represents the amount of energy deposited in each of the scintillating bars in the detector with dimensions of 6 mm $\times$ 3 mm $\times$ 96 mm.

The trigger rate for neutrons was 0.047 Hz on average and 1.7 Hz over the South Atlantic Anomaly (SAA) region, the latter being about 36 times higher than in any other region.

Here we briefly describe the photon detection. The detector has a sensitivity for low energy photons. Photons are converted into the electron and positron pairs in the sensor. However, in case that the converted electrons possess energy higher than 30 MeV, they will penetrate the inner sensor and enter into one of the plates of the anti-counter. Therefore they will be rejected by the anti-counter. Electrons possessing energy between 2.5 MeV and 30 MeV can be detected by the internal sensor as a thin track. Using the information of the ionization loss in each scintillating bar ($-dE/dX$), they are separated from the neutron converted protons.

5 Solar neutrons associated with M-class solar flares

According to the calculations of Imaida et al. (1999) and Watanabe (2005), the typical frequency of detection events due to solar neutrons is expected to be in the range 10 – 1000 Hz in the NEM. If the solar neutron flux associated with flares is proportional to the X-ray flux measured by the GOES satellite, it may be possible for our detector to see solar neutrons from even M-class flares. As mentioned earlier, the background rate is quite low at 0.047 Hz, so it is possible to detect all solar neutrons exceeding this level.

Since September 2009, no solar flares with intensities above X-class have occurred. However, during the period 6–8 February 2010, 4 large M-class flares were observed. Therefore, we analyzed the NEM data recorded at that time. Fortunately, during all 4 peaks in the X-ray intensity, the satellite was flying over the daylight side of the Earth. The peaks in X-ray intensity observed by the GOES satellite were at 6 February, 18:59 UT (M2.9); 7 February, 02:34 UT (M6.4); 8 February, 07:53 UT (M4.3) and 8 February, 13:47 UT (M2.0). Although we carefully searched the NEM records, there was no evidence of the arrival of neutrons from the Sun during any of these periods.

6 Conclusions

A new solar neutron detector was launched on 16 July 2009 by the space shuttle Endeavour, and began operation on the ISS on 25 August 2009. The sensor has since functioned very well and has measured neutrons both from the ISS module itself and albedo neutrons from the Earth, and has been fully capable of identifying the direction of the incident neutrons. The anti-counter system has worked effectively, allowing a high S/N ratio to be obtained. In addition, the energy spectrum of neutrons in the space environment of the ISS was measured. The trigger rate of neutrons was found to be 0.047 Hz. We also attempted to identify neutrons associated with the M-class solar flares that occurred on 6 and 8 February 2010, but no clear signals could be identified. Neverthe-

less, the results obtained in the early stages of operation of the system testify to its high potential to detect weak signals of solar neutrons induced by solar flares when they are produced.

Acknowledgements. The authors acknowledge the crew of the space shuttle Endeavor who have successfully mounted the SEDA-NEMdetector on the ISS Kibo exposed facility. We also extend thanks to the members of the Tsukuba operation center of Kibo taking the SEDA-NEM data everyday. The authors also acknowledge Dr Osamu Okudaira (JAXA) who has kindly made Monte Carlo calculations of the acceptance for us.

Edited by: K. Scherer
Reviewed by: two anonymous referees

References

Bütikofer, R., Flückiger, E. O., Muraki, Y., Matsubara, Y., Sako, T., Tsuchiya, H., and Sakai, T.: The upgrade solar neutron detector at Gornergrat, in: Proc. 27th ICRC (Hamburg), 8, 3053–3055, 2001.

Chikaoka, R.: Minutes of the 12th Space Development, Committee of the Ministry of Education, Science and Culture (chaired by the Minister R. Chikaoka), Report Nos. 13-1 and 12-3, 1997. (The Committee met on 9 April, 1997.)

Chinnery, M. A.: Solar Geophysical Data, National Geophysical Data Center, Bolder, Colorado, 543, 151–157, 1989.

Chupp, E. L., Debrunner, H., Flückiger, E., Forest, D. J., Golliez, F., Kanbach, G., Vestrand, W. T., Cooper, J., and Share, G.: Solar neutron emissivity during the large Solar flare on 3 June 1982, Astroph. J., 318, 913–925, 1987.

Doke, T.: Radiation hazard for the astronauts who stay for long time in the space, Science Asahi, 9, 38–43, 1997.

González, L. X., Sánchez, F., and Valdés-Galicia, J. F.: Geant4 simulation of the solar neutron telescope at Sierra Negra, Mexico, Nucl. Instr. Meth. A, 613, 263–271, 2010.

Imaida, I., Muraki, Y., Matsubara, Y., Masuda, K., Tsuchiya, H., Hoshida, T., Sako, T., Koi, T., Ramanamurthy, P. V., Goka, T., Matsumoto, H., Omoto, T., Takase, A., Taguchi, K., Tanaka, I., Nakazawa, M., Fujii, M., Kohno, T., and Ikeda, H.: A new tracking satellite-borne solar neutron detector, Nucl. Instr. Meth. A, 421, 99–112, 1999.

Koga, K., Goka, T., Matsumoto, H., and Muraki, Y.: Energy Resolution of the Solar Neutron Detector by the SEDA-AP on board JEM of ISS, in: Proc. 21st ECRS (Kosice, Slovakia) edited by: Kudela, K., Kiraly, P., and Wolfendale, A., 199–200, 2008.

Koga, K., Goka, T., Matsumoto, H., Muraki, Y., Obara, T., and T. Yamamoto, T.: Energy Determination of Solar Neutrons by the SEDA-AP on board JEM of ISS, 31st ICRC (Lodz, Poland), 831, SH1.3, 2009.

Moser, M. R., Flückiger, E. O., Ryan, J. M., Macri, J. R., and McConnel, M. L.: A fast neutron imaging telescope for inner heliosphere missions, Space Res., 36, 1399–1405, 2005.

Muraki, Y., Tsuchiya, H., Fujiki, K., Masuda, S., Matsubara, Y., Menjyo, H., Sako, T., Watanabe, K., Ohnishi, M., Shiomi, A., Takita, M., Yuda, T., Katayose, Y., Hotta, N., Ozawa, S., Sakurai, T., Tan, Y. H., and Zhang, J. L.: A new solar neutron telescope in Tibet and its capability examining by the 1998 November 28th event, Astropart. Phys., 28, 119–131, 2007.

Shibata, S.: Propagation of solar neutrons through the atmosphere of the Earth, Geophys. Res., 99, 6651–6665, 1994.

Watanabe, K.: Solar neutron events associated with large solar flares in Solar cycle 23, in: Proc. Cosmic Ray Res. section of Nagoya University, edited by: Muraki. Y., 46-2, 1–249, 2005.